

# 3D analysis of bone formation around titanium implants using micro computed tomography ( $\mu$ CT)

Ricardo Bernhardt<sup>a</sup>, Dieter Scharnweber<sup>a</sup>, Bert Müller<sup>b</sup>, Felix Beckmann<sup>c</sup>, Jürgen Goebbels<sup>d</sup>, John Jansen<sup>e</sup>, Henning Schliephake<sup>f</sup>, Hartmut Worch<sup>a</sup>

<sup>a</sup>Max Bergmann Center for Biomaterials, Technische Universität Dresden, D-01062, Germany;

<sup>b</sup>Computer Vision Laboratory, ETH Zürich, CH-8092 Zürich, Switzerland;

<sup>c</sup>GKSS-Forschungszentrum, D-21502 Geesthacht, Germany;

<sup>f</sup>Bundesanstalt für Materialforschung und -prüfung, D-12205 Berlin, Germany;

<sup>e</sup>Department of Biomaterials, Radboud Universiteit Nijmegen, 6500 HB Nijmegen, Netherlands;

<sup>f</sup>Department of Oral and Maxillofacial Surgery, George-Augusta University, D-37027 Göttingen, Germany

## ABSTRACT

The quantitative analysis of bone formation around biofunctionalised metallic implants is an important tool for the further development of implants with higher success rates. This is, nowadays, especially important in cases of additional diseases like diabetes or osteoporosis. Micro computed tomography ( $\mu$ CT), as non-destructive technique, offers the possibility for quantitative three-dimensional recording of bone close to the implant's surface with micrometer resolution, which is the range of the relevant bony structures. Within different animal models using cylindrical and screw-shaped Ti6Al4V implants we have compared visualization and quantitative analysis of newly formed bone by the use of synchrotron-radiation-based CT-systems in comparison with histological findings. The SR $\mu$ CT experiments were performed at the beamline BW 5 (HASYLAB at DESY, Hamburg, Germany) and at the BAMline (BESSY, Berlin, Germany). For the experiments, PMMA-embedded samples were prepared with diameters of about 8 mm, which contain in the center the implant surrounded by the bony tissue. To (locally) quantify the bone formation, models were developed and optimized. The comparison of the results obtained by SR $\mu$ CT and histology demonstrates the advantages and disadvantages of both approaches, although the bone formation values for the different biofunctionalized implants are identical within the error bars. SR $\mu$ CT allows the clear identification of fully mineralized bone around the different titanium implants. As hundreds of virtual slices were easily generated for the individual samples, the quantification and interactive bone detection led to conclusions of high precision and statistical relevance. In this way, SR $\mu$ CT in combination with interactive data analysis is proven to be more significant<sup>1</sup> with respect to classical histology.

**Keywords:** Micro computed tomography, synchrotron radiation, titanium implants, osseointegration, 3D analysis

## 1. INTRODUCTION

Of the methods that are available to characterize the bone formation process around implants, light microscopy is still the most widely used. An excellent lateral picture resolution is characteristic for this technique. In addition, with help of histomorphometry, quantitative data can be obtained. The two dimensional information as represented by the histological sections is then extrapolated to the three dimensional tissue structure by analyzing various sections of the same sample. However, such an extrapolation can result in incorrect information, since loss of large quantities of tissue (up to 300  $\mu$ m) is not uncommon during the sectioning of hard tissue-implant samples. For the quantification of mineralized bone (density or trabecular structure), micro computed tomography ( $\mu$ CT) has already been shown to be a very powerful technique.  $\mu$ CT has the ability to determine in a non-destructive way the bone formation around the implants with maintenance of a high spatial resolution and with minimal

---

Further author information: (Send correspondence to R.B.)

R.B.: E-mail: Ricardo.Bernhardt@tu-dresden.de, Telephone: +49 (0)351 463 39388

sample preparation. As a result, virtual cuts with identical resolution in any direction can be generated from  $\mu$ CT tomograms. However, the attenuation coefficients of bone and titanium, which is a widely used material for load bearing implants, differ significantly from each other. This can result in a lot of "noise" (scattering), which is present in the  $\mu$ CT image as a layer around the implant body. This effect becomes even enhanced during the first stages of bone formation when the difference in x-ray absorption is further increased because the newly formed tissue is not fully mineralized and thus composed mainly of light elements. Consequently, the visualization of the interface is complicated and a quantitative evaluation becomes difficult.<sup>2,3</sup> Some of these problems can be avoided by using synchrotron radiation micro tomography (SR $\mu$ CT).<sup>4</sup> Due to the monoenergetic and nearly parallel distribution of x-rays in SR $\mu$ CT, the so called "beam hardening effect" at the implant surface as well as scattering effects can be avoided. This leads to a higher sensitivity of bone detections near the implant surface. In this paper two exemplary titanium implant models will be presented to show the potential of this technique for the analysis of osseointegration with high statistical relevance.

## 2. MATERIALS AND METHODS

### 2.1. Implant design and biofunctionalization

In the first example cylindrical titanium implants with a diameter of 4 mm and a length of 12 mm were used. To clearly define a region of bone formation, two incisions with a width of 2.5 mm and a depth of 0.7 mm were cut into the titanium surface (Fig. 1A). For a second animal model modified screw titanium implants with a diameter of 4 mm were used (Fig. 2A). All implants were sandblasted with 250  $\mu$ m corundum and cleaned with 1% Triton X-100, acetone, and 96% ethanol, rinsed with distilled water, and air dried. The surfaces of the cylindrical implants were (1) uncoated (Ref), (2) collagen type I coated (Coll1),<sup>5</sup> (3) collagen type III coated (Coll3),<sup>5</sup> and (4) covered with peptide molecules (Pep).<sup>6</sup> The titanium screw implants with a machined surface were covered (1) with a combined hydroxyapatite and mineralized collagen coating<sup>6</sup> and (2) with a collagen I and chondroitin sulphate (CS) coating onto which bone morphogenetic protein 2 (BMP2) molecules were immobilized.<sup>7</sup>

### 2.2. *In vivo* experiments

The femur of sixteen healthy mature (2-4 years of age) female Saanen goats weighing about 50 kg were used for the implantation of the cylindrical implants.<sup>1</sup> Therefore a longitudinal incision of 4 mm was made on the medial surface of the left and right femur. Implantation periods were 5 and 12 weeks. The modified screw implants were implanted in the mandible of ten adult female foxhounds for 4 and 12 weeks.<sup>7</sup>

### 2.3. SR $\mu$ CT measurements

After retrieval and embedding 16 cylindrical samples (diameter = 8 mm, length = 15 mm) with titanium implants and the surrounding hard tissue from the goat experiment were used for the SR $\mu$ CT experiments. At HASYLAB (Hamburg, Germany) beam line BW5 monochromatic parallel x-ray was used. The photon energy was adjusted to 60 keV with a double-bent Laue-monochromator (Si-111 reflex). Behind the sample the attenuated x-rays were transformed by a single crystal (CdWO<sub>4</sub>) fluorescence screen into visible light, which was magnified to a CCD-camera (KX2 by Apogee Instruments, Inc.). The samples were measured under 720 different angles using an image size of 1274 x 1274 pixels (pixel size: 6.8 x 6.8  $\mu$ m). From the dog experiment 8 screw implants (two for each time and modification) with surrounding bone were embedded in methylmethacrylate and prepared with a diameter of about 8 mm, containing the implant nearly centered within the bony tissue. At the BAMline (BESSY II, Germany) the x-ray energy was set to 50 keV with the help of the installed double multilayer monochromator. With the CCD detector (VersArray:2048B, Princeton Instruments) 720 projections with an image size of 2048 x 2048 pixels and an effective pixel size of 3.5  $\mu$ m (zoom optics combined with CCD chip's pixel size) were obtained. A filtered back projection algorithm was used to obtain the three-dimensional data of x-ray absorption for the samples.

## 2.4. Analysis procedure

The extraction of bone-related absorption values in the SR $\mu$ CT tomograms was based on absorption histograms obtained with the image analysis software (ImageJ, National Institutes of Health, USA; VGStudioMax 1.1, Volume Graphics GmbH, Heidelberg, Germany). The various components in the tomograms were separated with an intensity-based gray level distribution threshold. Remaining image noise, which derives from the overlap of the gray levels of tissue and embedding material, was reduced with a structural image filter (ImageJ, noise/despeckle) retaining the overall bone structure.

In order to determine the amount of newly formed bone, the cavities in the implant were selected as the volume of interest (VOI) (Figure 1C and Figure 2B).

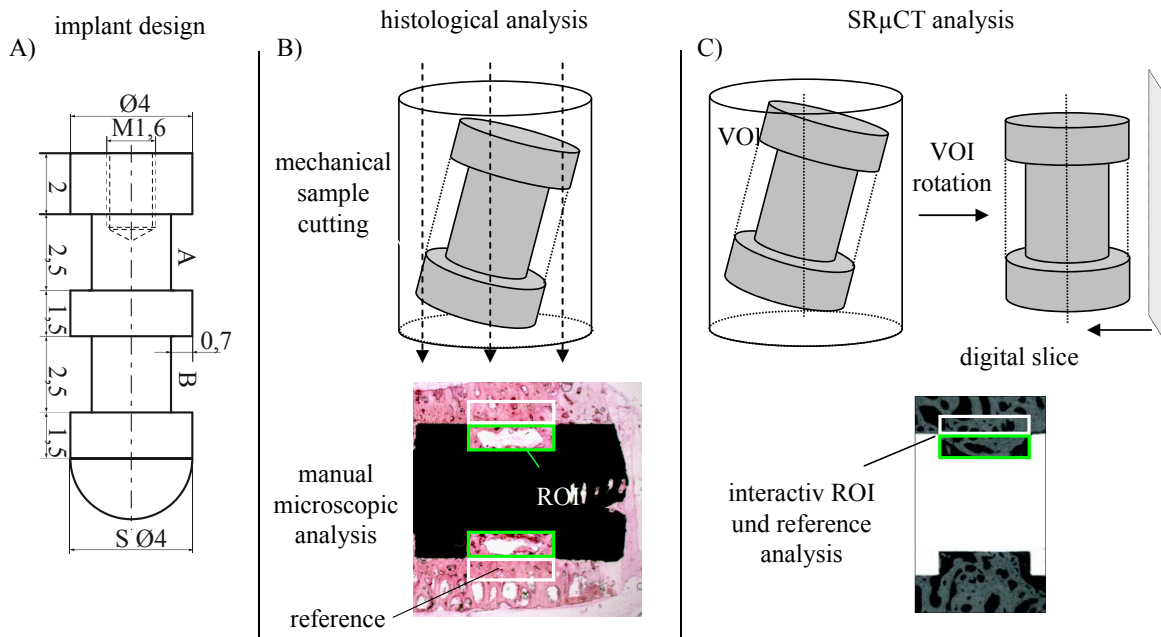


**Figure 1.** A) Schematic view of the cylindrical implant with two cavities. B and C) histological and SR $\mu$ CT-analysis procedure for the cylindrical implants. The volume of interest (VOI) is set to the cavities. The bone amount in a reference area above the VOI is calculated to take the surrounding bone quality into account.

As the implant axis in the samples is not fully adjusted to the z-axis of the  $\mu$ CT tomogram, a spatial reorientation of the longitudinal implant axis was done to position the ROI for the automatic slice scanning (cp. Figure 1C). The implant adjustment was carried out comparing the implant position at the top and the bottom slices to calculate the two transformation angles. The rotation of the  $\mu$ CT tomogram was done with an ImageJ plug-in (TransformJ v2.1, Copyright© by Erik Meijering, Rotterdam, The Netherlands). For the detailed comparison of accumulated bone the tomograms were sliced as subsequently done by histology (Figure 1B). Because of the different local bone structures, the reference area for each slice as shown in Figure 1C and Figure 2B was used, which corresponds about 1.5 x ROI-diameter. Due to the symmetric implant design, the binary slice stacks containing the bony structure could be projected (ImageJ, z-project). The resulting image divided by the certain absorption values is the normalized slice along the implant axis, which gives rise to an image containing floating-point values between zero (absence of bone values) and one (bone values at each point along the implant). Note that the implant is discarded in the resulting image.

For the histological investigation non-decalcified sections of the samples with a thickness of 30 to 70  $\mu$ m perpendicular through their long axis were prepared. The vertical resolution was about 1 mm. The resulting

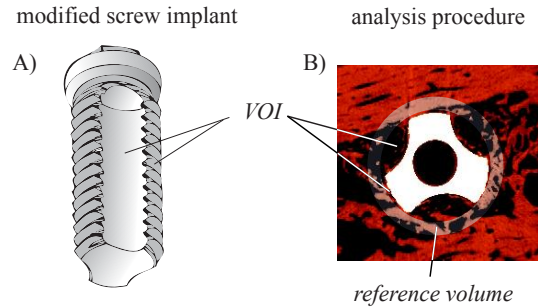


**Figure 2.** A) Schematic view of the modified screw implant. B) Analysis procedure for the measurement of mineralized bone inside the grooves in relation to a reference of the surrounding bone density.

slices were surface stained with alizarin-methylene-blue and von Kossa stain. To view the whole tissue around the implants from each slice micrographs with an image size of 900 x 600 pixels (pixel size: 12.6  $\mu\text{m}$ ) were taken.

The significance of differences in bone formation for the goat experiment were tested with a mixed multi factor analysis (linear model of the variance) using the SAS/STAT software (SAS Inst. Inc., Cary, NC). The parameters surface state, implantation time and location, including the interaction between implantation time and material, were investigated. The found mean values were 'Tukey adjusted'. Differences in bone formation around the screw implants were tested with an independent samples t-test. The significance level was defined as  $p < 0.01$ .

### 3. RESULTS AND DISCUSSION

The filtered 3D reconstructions (Figure 3 and Figure 4) obtained from the SR $\mu$ CT measurements at HASYLAB (BW5) and BESSYII (BAMline) show a clear contrast between the absorption values of mineralized bone and the titanium implant. Image artifacts usually found nearby the high absorbing titanium, are not visible. These graphics provide adequate information on the bone-implant interface and also suggest development of 3D image analysis modules to quantify the spatial bone amount around the implants. With the integration of thresholded values for mineralized bone along the implant z-axis of the SR $\mu$ CT volume preferred zones of bone formation could be visualized (Figure 5 and Figure 6). In the goat model the newly formed bone is mainly visible at the inner sides of the implant cavities. For the screw implants the highest amount of mineralized bone is found in the screw thread and after 12 weeks at the surface of the grooves.

The SR $\mu$ CT-analysis of the cavities in cylindrical implants shows differences in bone formation for the healing time and the surface modification. After 5 weeks the analyzed mineral bone volume differs with: Ref (27.5%, SD = 6.0%), Koll1 (39.2%, SD = 7.4%), Koll3 (34.6%, SD = 8.3%) and Pep (33.5%, SD = 4.2%). A general increase of mineralised bone was analysed after 12 weeks with: Ref (40.6%, SD = 7.0%), Koll1 (61.8%, SD = 12.4%), Koll3 (54.0%, SD = 10.0%) and Pep (49.1%, SD = 7.2%). With the mixed multi factor analysis the increase of bone formation for all implant modifications was found to be not significant ( $p < 0.01$ ). On the other hand, inside a given implantation time significant differences in bone formation between the surface modifications were found (Figure 7).

Both at 5 and 12 weeks of implantation, the differences between the various coatings and the reference material were statistically significant ( $p < 0.01$  for all coatings). Also the differences between the various coatings were significant ( $p < 0.01$ ) except between the 5 week peptide immobilized and collagen type III implants, and between the 12 week collagen type I and collagen type III implants. The statistical testing of the histological data revealed that no significant differences in bone formation between the implantation time and surface state existed ( $p < 0.01$ ).

For the screw implants after 4 weeks no significant differences ( $p = 0.15$ ) in bone formation between the coating with BMP2 (32.7%, SD = 10.9%) and mineralized collagen (31.4%, SD = 14.2%) was found. After 12 weeks the

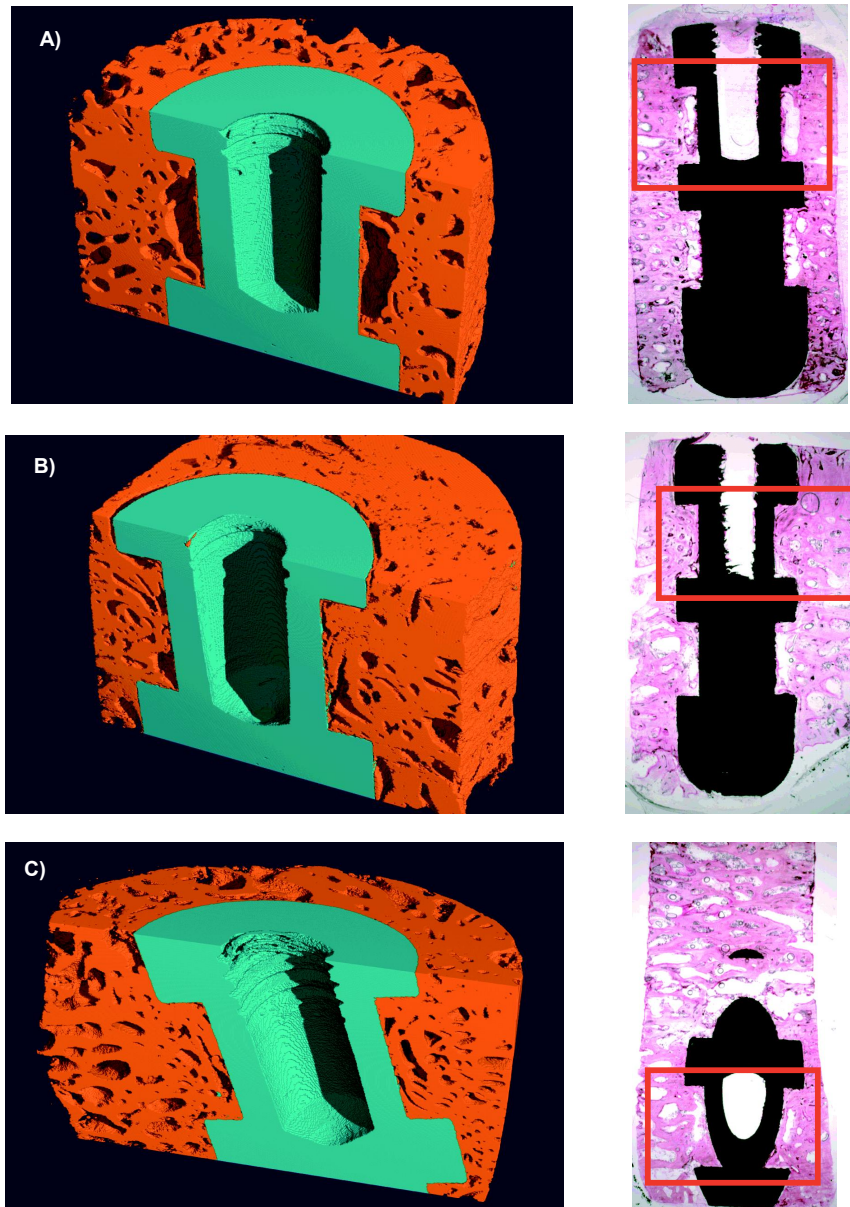


**Figure 3.** SR $\mu$ CT visualization of mineralized bone (orange) and titanium implant (cyan) after a healing time of 12 weeks for A) an uncoated implant, B) implant coated with collagen type I and C) an implant coated with collagen type III. The virtual slices in the SR $\mu$ CT-volume were correlated to histological micrography at nearly the same sample position (right side, red box) and demonstrate the good morphological agreement

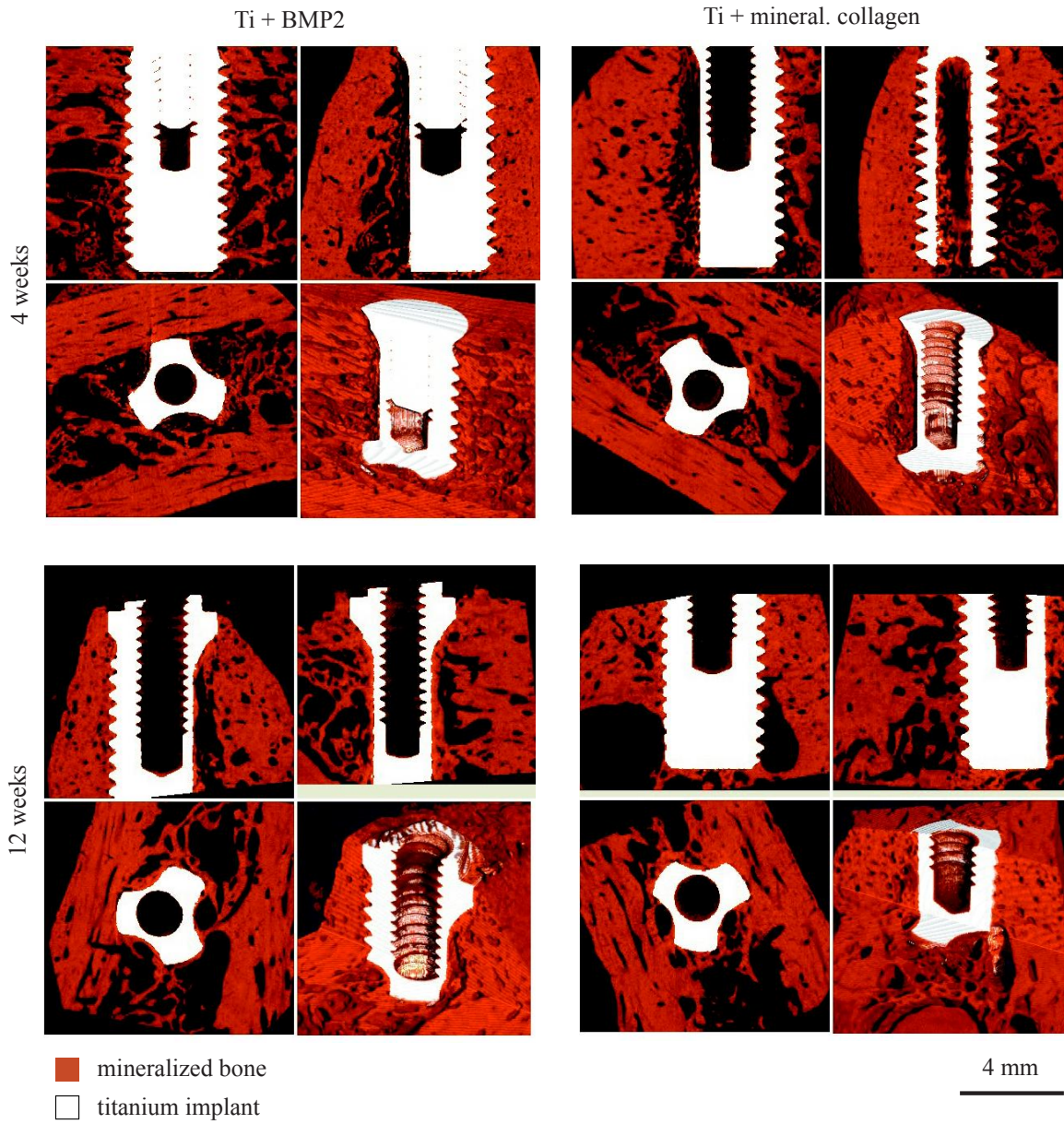


**Figure 4.** SR $\mu$ CT-visualization of absorption values around biofunctionalized titanium screws, measured at the BAMline (BESSYII, Berlin, Germany) with a photon energy of 50 keV.

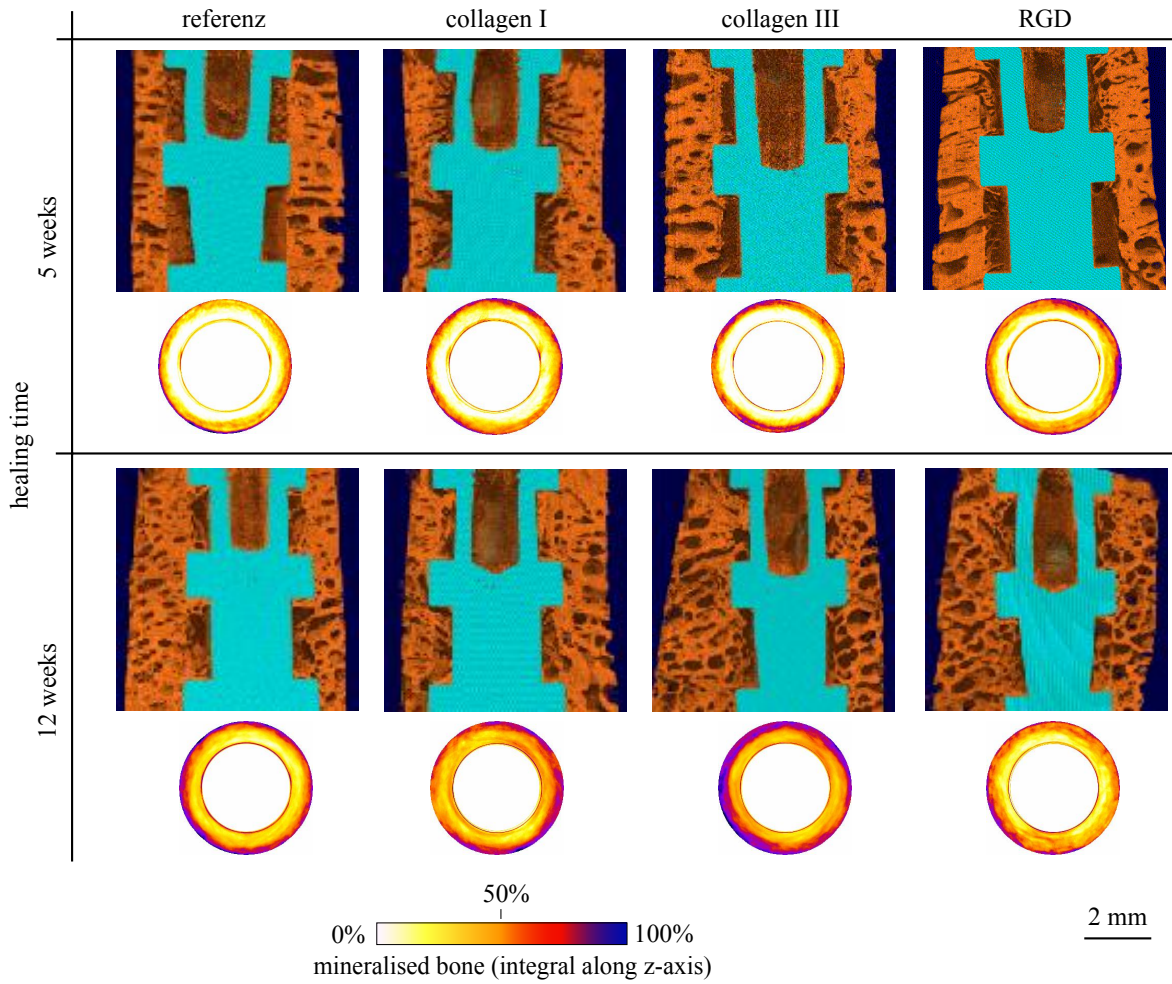


**Figure 5.** 3D Visualization of the mineralized bone inside the cavities of the biofunctionalized surfaces after a healing time of 5 and 12 weeks. The image below each 3D-visualization shows the integral amount of mineralized bone for all slices along the z-axis inside the cavities.

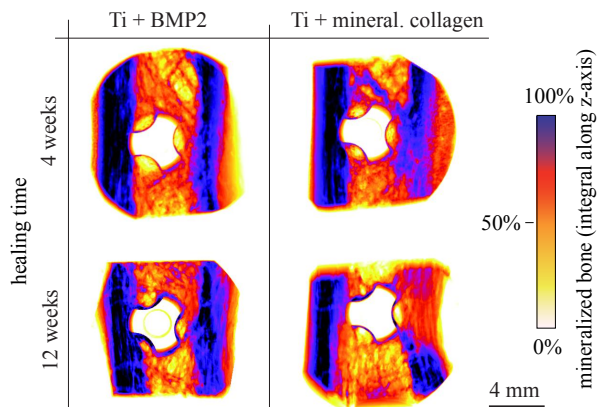


**Figure 6.** Absorption values for mineralized bone integrated along the z-axis of the SR $\mu$ CT-volume. After a healing time of 12 weeks inside the implant thread the highest amount of bone formation could be visualized for the BMP2 coating.

increase in bone formation for both coatings were highly significant ( $p < 0.001$ ) with a bone volume of 53.3% (SD = 13.0%) for BMP2 and 40.2% (SD = 19.0%) for mineralized collagen. Within a healing time of 12 weeks the bone volume inside the VOI was significant higher for BMP2 (Figure 8).

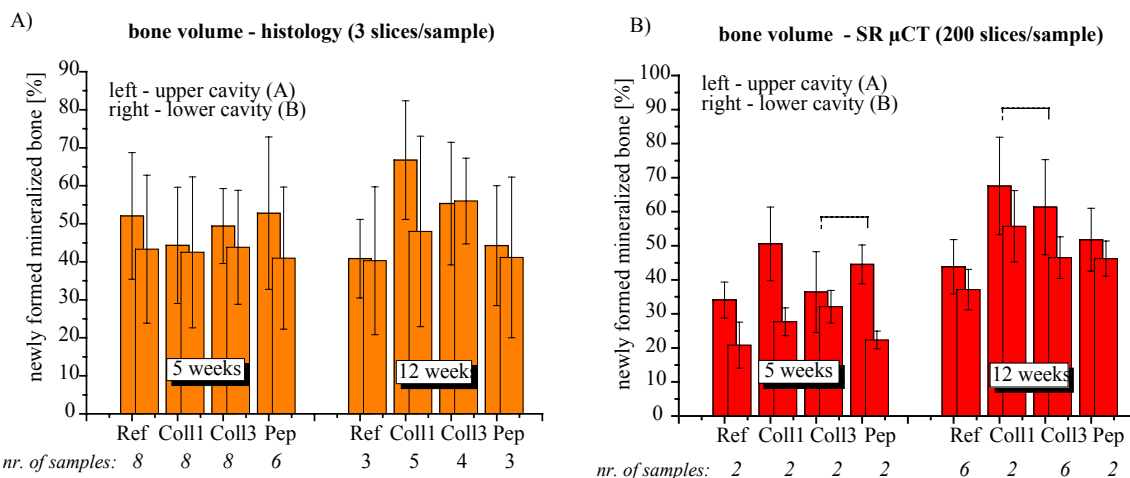


**Figure 7.** (A) Analysis of bone values inside the cavities from histological micrographs. No significant differences between the surface states could be found. (B) Analysis of bone volume from SR $\mu$ CT data. For a given implantation time, all coatings differed significantly ( $p < 0.01$ ) except those connected. No significant differences were found between materials at different healing times.

SR $\mu$ CT allows for a clear visualization of fully mineralized bone around the implants, as a very high number of slices can be generated per sample. As a consequence, the subsequent quantification and semi-automatic bone detection lead to a high precision of the results for each sample. A drawback is the time required for measuring, making it necessary to analyse a smaller sample number than would be desirable, as well as the limited availability of synchrotron sources for the  $\mu$ CT measurements. Although the preparation of the SR $\mu$ CT

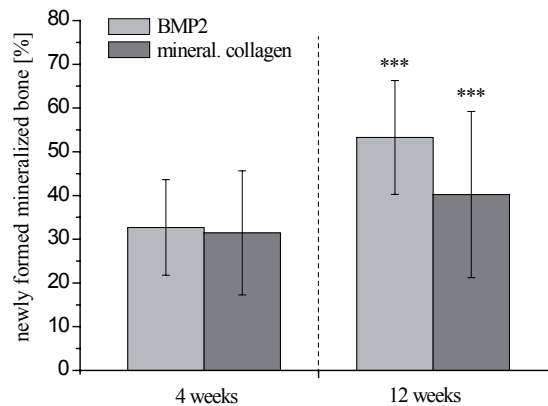


**Figure 8.** Results of the quantification for newly formed bone volume around the screw implants from SR $\mu$ CT information. After a healing time of 12 weeks the biofunctionalized implants show a highly significant increase ( $p < 0.001$ ) of bone formation, which is for the BMP2 coating significant higher than for the mineralized collagen coating.

samples is easier than the preparation of the histological ones, some restrictions have to be taken into account when evaluating the results. Because of similar x-ray absorption for the used histological embedding material and the not completely mineralized bone, a separation of these components can be difficult. As a consequence the  $\mu$ CT measurement has to be arranged prior to the histological embedding. The advantage of histological imaging is still the superb lateral resolution and the visualization of biochemical tissue properties. On the other hand, in terms of statistical relevance, visualization and quantification is more practicable with SR $\mu$ CT. Consequently, a combination of classical histology with SR $\mu$ CT can be a powerful instrument for an improved understanding of biological reactions around biofunctionalized implants.

## ACKNOWLEDGMENTS

This study was supported by the Bundesministerium für Bildung und Forschung (BMBF) and the Deutsche Forschungsgesellschaft (DFG). The authors thank Prof. Dr. Rainer Koch, Institut für Medizinische Informatik und Biometrie, Medizinische Fakultät Carl Gustav Carus, TU Dresden for valuable assistance in statistical analysis. The authors also thank Jacky den Bakker and Jan-Paul van der Waerden, Department of Biomaterials, UMC Nijmegen for their extensive assistance in the histological sectioning and evaluation. The financial support of these presentation by the "Gesellschaft von Freunden und Förderern der TU Dresden e.V." is kindly acknowledged.

## REFERENCES

1. R. Bernhardt, J. van den Dolder, S. Bierbaum, R. Beutner, D. Scharnweber, J. Jansen, F. Beckmann, and H. Worch, "Osteoconductive modifications of ti-implants in a goat defect model: characterization of bone growth with sr muct and histology," *Biomaterials* **26**(16), pp. 3009–19, 2005.
2. L. Sennerby, A. Wennerberg, and F. Pasop, "A new microtomographic technique for non-invasive evaluation of the bone structure around implants," *Clin Oral Implants Res* **12**(1), pp. 91–94, 2001.
3. H. Van Oosterwyck, J. Duyck, J. Van der Sloten, G. Van der Perre, J. Jansen, M. Wevers, and I. Naert, "Use of microfocus computerized tomography as a new technique for characterizing bone tissue around oral implants," *J Oral Implantol* **26**(1), pp. 5–12, 2000.
4. R. Bernhardt, D. Scharnweber, B. Müller, P. Thurner, H. Schliephake, P. Wyss, F. Beckmann, J. Goebbels, and H. Worch, "Comparison of microfocus- and synchrotron x-ray tomography for the analysis of osteointegration around ti6al4v-implants," *Eur Cell Mater* **7**, pp. 42–51, 2004.

5. S. Bierbaum, U. Hempel, U. Geissler, T. Hanke, D. Scharnweber, K. Wenzel, and H. Worch, "Modification of ti6al4v surfaces using collagen i, iii, and fibronectin. ii. influence on osteoblast responses," *J Biomed Mater Res* **67A**(2), pp. 431–8, 2003.
6. S. Rössler, D. Scharnweber, H. Worch, A. Sewing, and M. Dard, "Biomimetic coatings functionalized with adhesion peptides for dental implants," *J. Mater. Sci.: Mater. in Medicine* **12**, pp. 871–877, 2001.
7. H. Schliephake, A. Aref, D. Scharnweber, S. Bierbaum, S. Roessler, and A. Sewing, "Effect of immobilized bone morphogenic protein 2 coating of titanium implants on peri-implant bone formation," *Clin Oral Implants Res* **16**(5), pp. 563–9, 2005.